Artif Life Robotics (2014) 19:262–269
DOI 10.1007/s10015-014-0166-9

ORIGINAL ARTICLE

A new shooting algorithm for the search of periodic orbits

Keita Sumiya · Kazuhiro Kubo · Tokuzo Shimada

Received: 7 April 2014 / Accepted: 21 August 2014 / Published online: 26 September 2014

Abstract The periodic orbit theory gives the basic framework to study a quantum and classical correspondence. In this paper, we firstly report that we have found the existence of a certain surface, which we call the devil's staircase *surface*. Secondly, taking the advantage of some intriguing properties of this surface, we propose a new method to exhaustively search for periodic orbits in the anisotropic Kepler problem. Our method fully takes into account of an intriguing property of the initial value problem of the anisotropic Kepler problem, and it reduces the two-dimensional search into the one-dimensional search. Using this method, all of the periodic orbits up to the length $2N = 20$ (altogether 19284 distinct periodic orbits) have been successfully obtained, which exceeds the world record of 76 periodic orbits up to $2N = 10$.

Keywords Quantum chaos · Anisotropic Kepler problem · Devil's staircase · Periodic orbit theory

This work was presented in part at the 19th International Symposium on Artificial Life and Robotics, Beppu, Oita, 22–24 January, 2014.

K. Sumiya · T. Shimada (✉)
Department of Physics, School of Science and Technology, Meiji University, 1-1-1 Higashimita, Tama, Kawasaki, Kanagawa 214-8571, Japan
e-mail: tshimada@gravity.mind.meiji.ac.jp

K. Sumiya
e-mail: ksumiya@gravity.mind.meiji.ac.jp

K. Kubo
Institut fuer Physik, Technische Universitaet Ilmenau, Weimarer Strasse 25, 98693 Ilmenau, Germany
e-mail: kazuhiro.kubo@tu-ilmenau.de

1 Introduction

For a chaotic system, it is important to consider how the quantum theory retains chaotic features of its classical theory. This becomes of practical importance with the advent of mesoscopic and nanoscale devices. The periodic orbit theory (POT) gives a crucial key to investigate this issue. It is a semiclassical quantization scheme applicable to the chaotic system constructed by Gutzwiller [1]. The core equation in the POT is the trace formula

$$\sum_n \frac{1}{E - E_n + i\epsilon} \approx \sum_{r\in \mathrm{PPO}} \frac{T_r}{\pi\hbar} \sum_{n\neq 0} \frac{\mathrm{e}^{in\left[\frac{S_r}{\hbar} - \frac{\pi}{2} l_r\right]}}{\sqrt{\det(M_r^n - 1)}} \tag{1}$$

where the LHS is given by quantum energy levels, while in the RHS, outer sum is taken over all primitive periodic orbits (PPOs) and inner sum counts the repetition of each PPO. T_r, S_r, and l_r denote the period, action, and Maslov index of the PPO, respectively, and M_r stands for the monodromy matrix of the PPO. In this way, the search for the periodic orbits (POs) is essential to pin down the quantum and classical correspondence.

To be specific, we consider the anisotropic Kepler problem (AKP), which is a variation of a hydrogen atom with the electron having an anisotropic mass tensor. The AKP is a superior model for investigating the quantum and classical correspondence for some following reasons. Firstly, the chaoticity of the AKP depends on only one parameter γ. Secondly, the AKP has become tractable in recent experiments. Thirdly, in the AKP with high mass anisotropy, there exists an orbit for any given binary code (coding theorem) [3, 4], and it is supposed to be unique (Gutzwiller's conjecture).

In this paper, we consider the two-dimensional AKP. We focus our attention to a two-dimensional surface hanged on

the initial value plane (Poincaré section in properly chosen canonical variables), with the height being calculated by the binary code of the orbit, which starts from every point of the Poincaré section. Now, suppose that we wish to find a particular periodic orbit with a given code. This means that we want the proper initial point that produces this PO. Given the coding theorem, it is in principle sufficient to locate the point(s) on the surface at the height of the code and seek the corresponding base point(s). If there turns out only one point, it is quite in keeping with the uniqueness conjecture. In practice, it is impossible to construct it with infinite resolution, but we can construct it with a sufficient resolution for the target POs. The basic theme in this report is how to search the POs strategically referring to the information embodied in the surface. Most importantly, we find that it is monotonic, indicating that the uniqueness conjecture is correct. Our surface is an extension of the devil's staircase considered by Gutzwiller [5], which is fractal and contains non-differentiable points. We call it 'Devil's Staircase Surface' (DSS).

From the next section, we are going to introduce the DSS, and using it, we propose a search algorithm for POs in the AKP, which is exhaustive.[1]

Our strategy, the reduction of a search space by the system regularities, should be useful in a wide range of problems.

2 Surface of the devil's staircase in the AKP

In the two-dimensional AKP with x-axis being heavy-axis, the Hamiltonian is

$$H = \frac{1}{2\mu}p_x^2 + \frac{1}{2\nu}p_y^2 - \frac{1}{\sqrt{x^2+y^2}} \quad (\mu \geq \nu, \mu\nu = 1), \tag{2}$$

where μ and ν are values for the mass anisotropy. At $\gamma \equiv \nu/\mu = 1$, the system is the usual Kepler problem, which is one of the most basic solvable problem in both quantum and classical mechanics. With increasing the mass anisotropy, the chaoticity becomes stronger. We choose $\gamma = 0.2$ where the classical system is known to be completely ergodic.

In what follows, we fix the energy at the standard value $E = -1/2$ thanks to the scaling property of the AKP

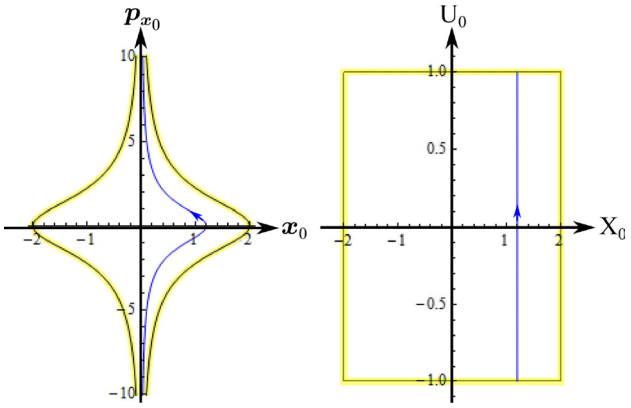

Fig. 1 The transformation of the initial value space ($E = -1/2$ fixed). The boundary of an initial-value-set in (x_0, p_{x_0}) space is the Lorentzian, while that one in (X_0, U_0) space is a *rectangle*. $r = 0$ is the sides $U_0 = \pm 1$ and the *center line* $X_0 = 0$ connecting the both sides

Hamiltonian [2]. At this choice of the energy, the set of all possible initial values (x_0, p_{x_0})—with y_0 set to zero to define the Poincaré surface of section—is a region

$$|x_0| \leq 2\left(1 + \frac{p_{x_0}^2}{\mu}\right)^{-1}, \quad -\infty < p_{x_0} < \infty, \tag{3}$$

shown in the left diagram of Fig. 1. In the Gutzwiller's coordinate system (X, U) [3] (with $U \to 2U/(\pi\sqrt{\mu})$)

$$X = x\left(1 + \frac{p_x^2}{\mu}\right), \quad U = \frac{2}{\pi}\arctan\left(\frac{p_x}{\sqrt{\mu}}\right), \tag{4}$$

the initial value space—the space of (X_0, U_0)—becomes

$$|X_0| \leq 2, \quad |U_0| < 1, \tag{5}$$

and it is a simple rectangle in the right of Fig. 1.

Consider an orbit which starts from an arbitrary initial value (X_0, U_0) and crosses the X-axis as $(X_0, X_1, X_2, \ldots)$. Let $a_i (= \pm 1)$ denotes the sign of X_i and construct a binary code $(a) \equiv (a_0, a_1, a_2, \ldots)$ for the orbit. In this way, any orbit can be labeled by a corresponding binary code. (Let us call this direction A). While this fact is trivially true, the reverse (call it direction B) is far from trivial. It has been shown by Gutzwiller [3] (and by Devaney [4] mathematically) that there is at least one orbit exists for a given binary code. The code of a periodic orbit must be a cyclic binary code

$$(a)_P = (a_0, \ldots, a_{2N-1})|_{a_{2N}=a_0} \tag{6}$$

because it must cross the X-axis even times to come back to the initial point with the same momentum. It is conjectured that there is only one periodic orbit for a given cyclic binary code—that is, the initial value (X_0, U_0) is unique.

[1] In [2], we restricted ourselves to a symmetric orbit search and showed that a simple shooting with full attention to the scaling property of the AKP supplies better convergence than a traditional search [1] based on the Hill's method in the restricted 3-body problem. The quantum physics issue was also briefly introduced. In this report, we treat a two-dimensional PO search which requires further considerations.

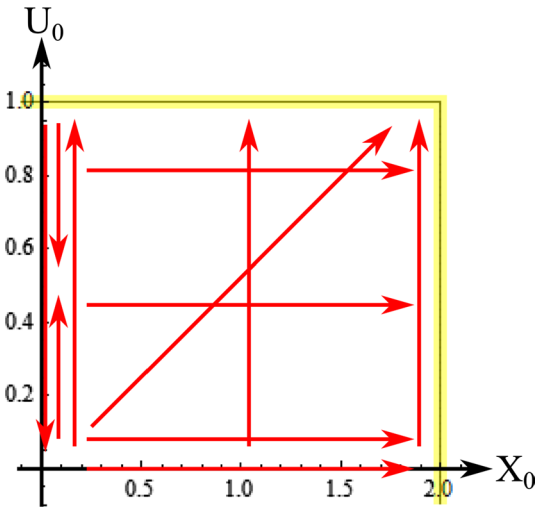

Fig. 2 Some increasing tendencies in the fundamental region. In the direction of *each arrow*, the number ζ increases

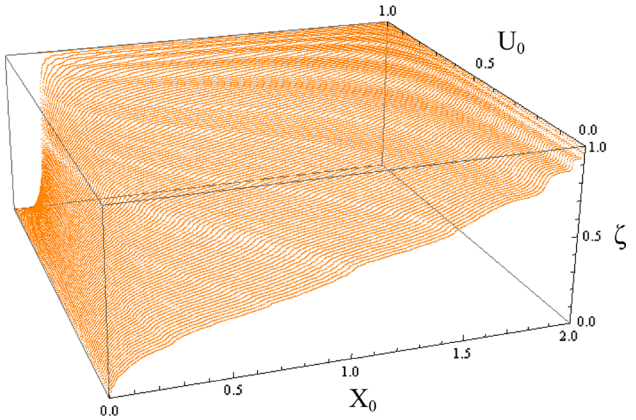

Fig. 3 The devil's staircase *surface*. 2000×100 grid points are set on the fundamental rectangle $[0, 2] \times [0, 1]$, orbits are tracked for the binary code starting from a_0 until $a_{i_{\max}=48}$ (the precision boundary for a double precision calculation), and then, $\zeta(X_0, U_0)$ are calculated from $(a_0, \ldots, a_{48})$

Here N is called the rank and $2N$ is the length of the PO. One can label a PO by its binary code or, alternatively, by the rank and the identification number (Id) within the rank.[2]

Back to direction A, let us calculate a number[3] by

$$\zeta(X_0, U_0) \equiv \sum_{i=0}^{\infty} \frac{1}{2^{i+1}} a_i(X_0, U_0) \tag{7}$$

and $a_0 \equiv 1$ to remove the redundancy. The curve $\zeta(X_0, U_0)$ at $U_0 \equiv 0$ was examined by Gutzwiller [5]. He found that it is monotonically increasing as a function of X_0, and it is fractal—it is a devil's staircase [6].

We have extended this devil's staircase curve of Gutzwiller into the U_0 direction and have numerically confirmed that it makes a surface with a remarkable structure as depicted in Fig. 2.

With increasing X_0 at any fixed U_0, the height of the surface $\zeta(X_0, U_0)$ monotonically increases. On the other hand, with increasing U_0 at fixed X_0, $\zeta(X_0, U_0)$ also monotonically increases except for very small X_0 ($\lesssim 0.15$). We exhibit the surface in Fig. 3.[4] We call this surface *the devil's staircase surface* (DSS).

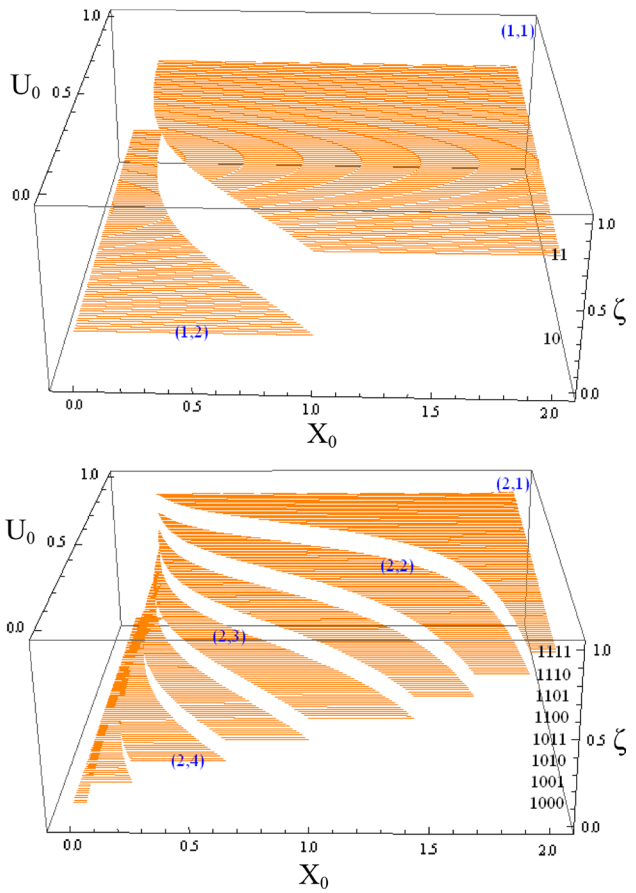

Fig. 4 The coarse-grained DSS with $N = 1$ in the *upper* and $N = 2$ in the *lower diagram*. The step height ζ is calculated by the $2N$ digit code using Eq. (8) after undoing the abbreviation (for instance, $(1001) \to (+1, -1, -1, +1)$). POs we found are indicated by their (N, Id) on the steps

[2] Due to the symmetry of the AKP Hamiltonian, distinct codes related by certain transformations may express essentially the same periodic orbits as analyzed in detail in [3]. Therefore, equivalent codes are classified into a class. The representative code for each class is the one which wins the highest ζ (Eq. (7)) among the class. Then, one compares the representatives and assigns identification numbers to them in the decreasing order of their ζs.

[3] While we can construct numbers for the future(ζ^f) and past(ζ^p) [3], we use only ζ^f in this paper, and we suppress the superscript f.

[4] We show the initial value space limited to the fundamental region $(X_0, U_0) \in [0, 2] \times [0, 1]$.

For the purpose of this report, a double precision computation is sufficient, which allows the best precision binary code $(a_0, a_1, a_2, \ldots, a_{i_{\max}=48})$. Figure 3 is the best surface in this precision, and it has 2^{48} steps—the finest step is invisible in the scale of the Figure. (In a rough estimate, the height of the figure must be 0.2 AU to present each step resolvable with 0.1 mm!)

We have so far discussed the DSS constructed by an infinite sum (within 49 digits truncation). Now, it is also very interesting to see how this DSS by infinite sum is built up by constructing the coarse-grained version

$$\zeta(X_0, U_0) \equiv \sum_{i=0}^{2N-1} \frac{1}{2^{i+1}} a_i(X_0, U_0). \tag{8}$$

Every step is then formed by such initial (X_0, U_0) that orbits from them evolve in the same code (corresponding to the height of the step) during the first $2N$ Poincaré sections. For the purpose of the coarse graining, any integer upper bound for the sum will do, but we have chosen here $2N-1$ in order to facilitate a comparison with the rank N POs (see Eq. 6). Since a_0 is fixed canonically to 1, there are 2^{2N-1} steps for the N coarse- grained DSS and the rank N POs (with the truncated code, i.e., Eq. 6 without the cyclic repetition) seat themselves on these steps. In Fig. 4, we show the coarse- grained DSS with $N = 1$ in the upper and $N = 2$ in the lower diagram. We also indicate the positions of POs (with the truncated height) on the respective surfaces (there are 2 (4) distinct POs in $N = 1 (N = 2)$. For our results up to $N = 10$, see Table 1).

With the increase of N, the number of steps increases and their widths are accordingly reduced, and at the infinite N limit, the final limiting surface is formed and the full—non-truncated—POs are on it. It is constructed by both cyclic (the ζ is rational) and non-cyclic (the ζ is irrational) ones. Can we select the periodic ones on the DSS? In the next section, we will solve this problem successfully and we compute the POs exhaustively up to $N = 10$.

3 Search of POs up to $2N = 20$

We describe below our search algorithm for a periodic orbit (call it the target-PO), labeled by a given cyclic binary code $\bar{a} \equiv (a_0 \equiv 1, a_1, \ldots, a_{2N-1})|_{a_{2N} \equiv a_0}$.

Preparation

The number $\tilde{\zeta}_{\rm PO}(\bar{a})$ for the target-PO is calculated[5] by

[5] The number $\tilde{\zeta}$ for the target-PO is also calculated by the cyclic binary code with 49 binary digits, just as we calculate the $\zeta(X_0, U_0)$ by 49 binary digits.

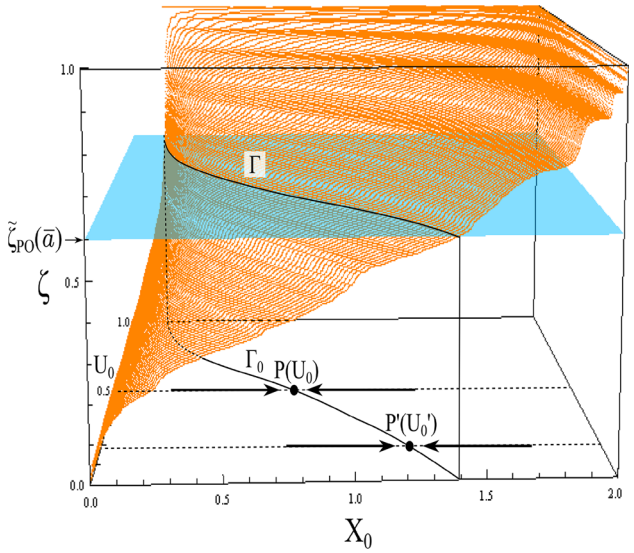

Fig. 5 An illustration of the first step—the search of the level line on the DSS with a height $\tilde{\zeta}_{\rm PO}(\bar{a})$. As exhibited in the *bottom*, we search a point $P(U_0)$ for each U_0 that satisfies at best the condition $\zeta(X_0, U_0) = \tilde{\zeta}_{\rm PO}(\bar{a})$, and they $(P(U_0), P'(U_0'), \cdots)$ altogether form the base level contour Γ_0

$$\tilde{\zeta}_{\rm PO}(\bar{a}) \equiv \sum_{i=0}^{\infty} \frac{1}{2^{i+1}} a_i. \tag{9}$$

Please do not confuse $\tilde{\zeta}_{\rm PO}(\bar{a})$ with $\zeta(X_0, U_0)$ defined by Eq. (7). $\tilde{\zeta}_{\rm PO}(\bar{a})$ is different from $\zeta(X_0, U_0)$. $\tilde{\zeta}_{\rm PO}(\bar{a})$ is defined independently from an initial value (X_0, U_0) (it is the target of the shooting), while $\zeta(X_0, U_0)$ is a function of (X_0, U_0) describing the DSS.

The first step :
Search for a level contour on the devil's staircase surface with a height $\tilde{\zeta}_{\rm PO}(\bar{a})$

Here we search for a level contour on the DSS with a height $\tilde{\zeta}_{\rm PO}(\bar{a})$. Figure 5 is a key map of the procedure for it. In the U_0 interval $[0, 1]$, we take equally spaced N_U points $U_i = i/N_U$, and on each $U_0 = U_i$ line, we search for the value of X_0 (a point P) so that the binary code of the orbit starting from (X_0, U_0) shares with the binary code $\bar{a}$ from a_0 to typically a_{40}.

Taking the advantage of the monotonically increasing property of the DSS at any fixed U_0 (see Fig. 2), we adapt a bisection method.

Consider an X_0 interval $[X_A, X_B]$ on a chosen U_0 line (selected by a do-loop) and calculate a number ζ_m at the midpoint X_m. Because we examine the fundamental region $(X_0, U_0) \in [0, 2] \times [0, 1]$, we choose the starting interval

as $[X_A, X_B] = [0, 2]$ (with the midpoint $X_m = 1$) and calculate the orbit from (X_m, U_0). Then, we calculate the number ζ_m for this orbit. Now, we determine the next interval from ζ_m; if $\zeta_m < \tilde{\zeta}_{\rm PO}$, then we replace X_A by X_m; otherwise we replace X_B by X_m. This gives the second interval. By repeating this procedure iteratively, we can squeeze the X_0 interval to a point $P(U_0)$.

Running this first step on all U_0s by the said do-loop, the base curve Γ_0 of the level contour Γ is generated (see Fig. 5). Any points on this contour Γ_0 are candidate initial points for the target-PO, because the binary code of the orbit from there agrees with the binary code $\bar{a}$ from a_0 up to typically a_{40}. We will see in the next step that the wanted initial point of the target-PO is only one point on this candidate curve.

The second step : Important observation

Here we report an important observation on the χ^2 function on the base level contour Γ_0. This is a prelude to the final step.

A chi-squared value is defined as a measure of the amount of the misfit between the initial (0th) and the final ($2N$th) Poincaré sections.[6]

$$\chi^2 \equiv (x_f - x_i)^2 + (y_f - 0)^2 + (p_{x_f} - p_{x_i})^2 + (p_{y_f} - p_{y_i})^2. \tag{10}$$

It is worth to note the difficulty of finding a PO by simply minimizing χ^2. To illustrate it, we show in Fig. 6 the χ^2 sampled by the 10^3 grid points in the U_0 interval $[0, 1]$ at fixed X_0. At a glance one finds that it is too jaggy to search the bottom. Although an adaptive shooting might work at the cost of large computing time, the exhaustive search for all of the POs will be impossible on this line.

Contrary to this, χ^2 curve sampled along the candidate curve Γ_0 is remarkably simple; it is a convex curve with only one bottom with χ^2 equals to 0 with an error of typically 10^{-10} as shown in Fig. 7. This point is nothing but the wanted initial point of the target-PO. The comparison between Figs. 6 and 7 succinctly shows that it is the curve Γ_0 if one does the search for a PO along a certain curve. We have confirmed that this superior property holds along any candidate curves for other POs.

The fact that the χ^2 curve turns out such a simple pattern is highly non-trivial. Furthermore, the unique existence of a bottom is nothing but the Gutzwiller's conjecture!

[6] The Poincaré section is defined by $y = 0$, and $y_i = 0$. But, for y_f, there remains inevitably finite y_f, because of the finite Δt in the integration procedure. We have applied a linear interpolation to improve the final time decision within $\Delta t = 10^{-4}$, and used supplemental integration within the last Δt to determine the final Poincaré section.

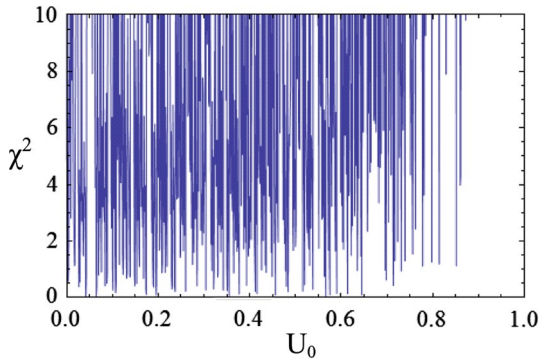

Fig. 6 The χ^2-plot along a line at $X_0 = 1$. The increment for U_0 is 10^{-3}. χ^2 is calculated in the $2N = 10$ case

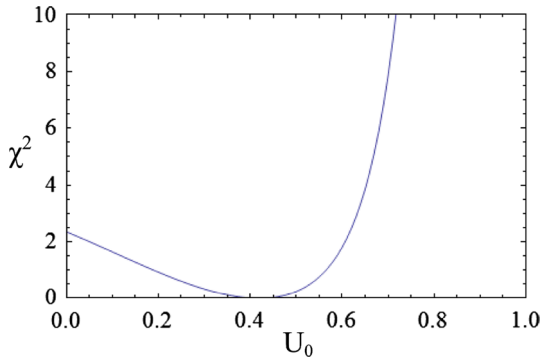

Fig. 7 The χ^2-plot along the candidate curve Γ_0 in the case of the PO ($2N = 10$, Id = 38). The increment for U_0 is here 10^{-2}

The third step : The PO search in the candidate curve

The final step is the search of the wanted initial point of a target-PO along the Γ_0 as illustrated in the key map in Fig. 8. Because the χ^2-curve is convex with a single bottom, we search for the point Q by the use of a standard trisection method.

Divide a U_0 interval $[U_A, U_B]$ into three equal segments by separation points U_1 and U_2 ($U_1 < U_2$). Searching out positions P_1 and P_2 on the candidate curve at a fixed U_1 and U_2, respectively, by the first step algorithm, we calculate χ^2 s at these positions. Because we work in the fundamental region, we choose the starting interval as $[U_A, U_B] = [0, 1]$ (with $U_1 = 1/3, U_2 = 2/3$), and calculate the orbit from P_1 and P_2. Then, we compare $\chi^2(P_1)$ with $\chi^2(P_2)$. If $\chi^2(P_1) < \chi^2(P_2)$, then we replace U_B by U_2; otherwise we replace U_A by U_1. This gives the second interval. By repeating this procedure iteratively, we search out the point Q on

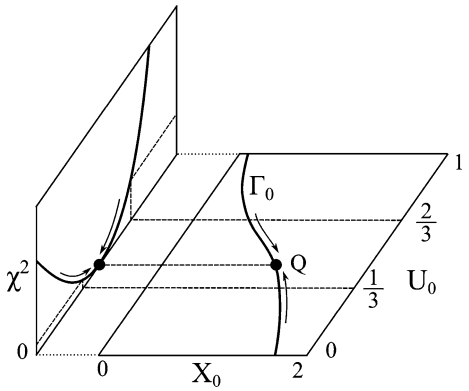

Fig. 8 An illustration of the third step. The candidate curve Γ_0 has been already obtained by the bisection procedure shown in Fig. 5, and the *curve in the left panel* shows the χ^2 value along Γ_0 (it is a simple convex curve with one minimum). The minimum χ^2 point Q (in fact $\chi^2 = 0$ for a PO) on Γ_0 can be obtained by a standard trisection method, and it gives us the wanted initial value (X_0, U_0) for the target-PO

Table 1 The number of all distinct periodic orbits which we have found by our numerical algorithm

The rank N	The number of POs
1	2
2	4
3	8
4	18
5	44
6	122
7	362
8	1162
9	3914
10	13648
Total	19284

This precisely agrees with the prediction given by the unique existence conjecture by Gutzwiller and the symmetry consideration [3, 8]

the candidate curve and there $\chi^2 \approx 0$. This completes our PO search algorithm. ———

Due to the symmetry of the Hamiltonian, AKP orbits may have symmetries; the symmetry with respect to the x -axis $(y \to -y)$, or y-axis, time-shift and time-reversal symmetries. If an orbit is obtained from the other one, one counts them the same. The number of distinct orbits after this identification is listed in Table 1.

Now we have all distinct periodic orbits in this list, altogether 19284 periodic orbits. This exceeds the previous world record up to $2N = 10$ (76 POs) [7].

In Fig. 9, we present three sample orbits with the rank $N = 10$ at $\gamma = 0.2$ and their characteristics in Table 2. Full profiles of 13648 periodic orbits at $N = 10$ are available:

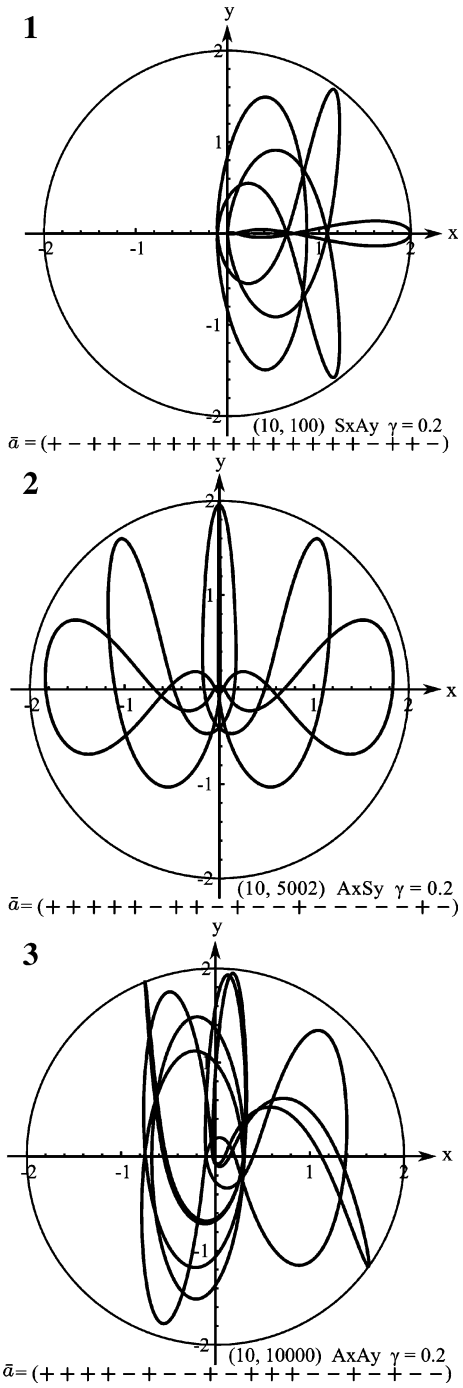

Fig. 9 Three sample periodic orbits with length $2N = 20$ in the (x, y) plane. Mass anisotropy $\gamma = 0.2$. We denote by S_x (A_x) that it is symmetric (asymmetric) under the x-transformation $(x \to x, y \to -y)$. **1** Id = 100, type-(S_xA_y), **2** Id = 5002, type-(A_xS_y), **3** Id = 10000, type-(A_xA_y). The *circle* exhibits the kinematical boundary

http://www.isc.meiji.ac.jp/~tshimada/arob2014/sumiya-kubo-shimada_arob2014_orbit-profiles.pdf

This is, to our knowledge, the first time appearance of $N = 10$ POs in the literature.

Table 2 The details of the sample POs in Fig. 9

Periodic Orbit (1)	
(N, Id)	(10, 100)
Symmetry	S_xA_y
X_0	0.8662601476594602
U_0	0.0000000000000000
Lyapunov exponent	19.36441255533023
Action	30.64876862775776
Binary code	$\overline{a} = (+-++-+++++++++++++-++-)$
Periodic Orbit (2)	
(N, Id)	(10, 5002)
Symmetry	A_xS_y
X_0	1.200325396087828
U_0	0.8860249568347829
Lyapunov exponent	17.46793360630122
Action	40.77425334607968
Binary code	$\overline{a} = (++++-++-+--+---------+-)$
Periodic Orbit (3)	
(N, Id)	(10, 10000)
Symmetry	A_xA_y
X_0	1.073770101110692
U_0	0.8065616216559989
Lyapunov exponent	14.31908020947697
Action	49.36092248823712
Binary code	$\overline{a} = (+++-+--+-++--+-+--)$

We list the followings; the rank N, Id, symmetry properties, initial values (X_0, U_0), Lyapunov exponent, action (= period at the choice $E = -1/2$), binary code. Initial values (X_0, U_0) listed in the table guarantee one more evolution of the full PO profile (i.e., 40 digits)

4 Conclusion

In this paper, we have reported our findings, especially the existence of the DSS, and presented an efficient and fail-safe PO search algorithm, which fully utilizes this DSS. The algorithm uses two intriguing properties we have found for the DSS;

(1) The number ζ (the height of the DSS) monotonically increases with increasing X_0 at fixed U_0.
(2) χ^2 value along the proper level of the DSS is a simple convex curve with only one bottom, where $\chi^2 = 0$ as required for a PO.

These two properties are fully consistent with the Gutzwiller's conjecture and support it. By our method, we have successfully obtained the exhaustive list of POs up to $2N = 20$, altogether 19284 POs. This gives a definitive support for the Gutzwiller's conjecture for the unique existence of the PO for a given binary.

We consider that our PO search is a successful example of an intelligent search of a solution in a complex problem. To illustrate our strategy, an analogy with the famous Born–Oppenheimer approximation (BOA) will be helpful. In the BOA, we solve out the molecule configuration by separating slow (nuclei) and rapid (electrons) modes. Firstly, nuclei are tentatively fixed, and the wave function of electrons are solved to give an effective potential between nuclei. Then, nuclei slow dynamics is solved with this potential. This inspires the importance of strategy in handling the problem of searching the solution. Do not contend with it as a whole; separate the modes in it and solve the interlink between them. Our success comes from the separation of two directions in the parameter space. In the first step, we have located the level contour, which amounts to discarding the direction of the rapid change of the chi-squared function. (Integrating out irrelevant modes is also the basic strategy in the renormalization group approach to find the phase transition.) In the third step, we have searched the PO position in the level contour, that is, within the slow direction.

Let us conclude by describing briefly the recent status after AROB 19.

(i) We have successfully shown that the DSS's property in Fig. 2 by mathematical induction for the iterated one-time map of AKP flow.
(ii) We have noticed that Gutzwiller showed future and past-level contours are produced by the collision orbits [5, 9]. The relation between two approaches is under scrutiny.
(iii) Future and past-level contours enclose the corresponding PO as noted in [9]. Despite the description there, we have found that this fact is useful for PO search even for the difficult $2N = 20$. Our strategic χ^2 procedure using a future contour is by far efficient.
(iv) Gutzwiller's approximation [10] for the action values of POs, using analogy with a certain spin system, works surprising well over all POs up to $2N = 20$.

These issues will be discussed elsewhere.

References

1. Gutzwiller MC (1971) Periodic orbits and classical quantization conditions. J Math Phys 12:343–358
2. Kubo K, Shimada T (2009) AKP energy levels by a simple shooting scheme for a periodic orbit. Artif Life Robot 14:557–561
3. Gutzwiller MC (1977) Bernoulli sequences and trajectories in the anisotropic Kepler problem. J Math Phys 18:806–823
4. Devaney RL (1978) Collision orbits in the anisotropic Kepler problem. Invent Math 45:221–251
5. Gutzwiller MC (1989) Multifractal measures and stability islands in the anisotropic Kepler problem. Phys D 38:160–171
6. Peitgen HO, Jürgens H, Saupe D (1992) Chaos and fractals: new frontiers of science. Springer, New York, pp 220–228
7. Gutzwiller MC (1981) Periodic orbits in the anisotropic Kepler problem. In: Proceedings of classical mechanics and dynamical systems. Marcel Dekker, New York, pp 69–90
8. Kubo K, Shimada T (2014) Periodic orbit theory revisited in the anisotropic Kepler problem. Prog Theor Exp Phys 023A0:1–19
9. Gutzwiller MC (1988) From classical to quantum mechanics with hard chaos. J Phys Chem 92:3154–3163
10. Gutzwiller MC (1980) Classical quantization of a Hamiltonian with ergodic behavior. Phys Rev Lett 45:150–153